An inertial range model for the three-point third-order velocity correlation

Henry Chang
Institute for Computational Engineering and Sciences, University of Texas at Austin, Austin, Texas 78712, USA

Robert D. Moser
Institute for Computational Engineering and Sciences and Department of Mechanical Engineering, University of Texas at Austin, Austin, Texas 78712, USA

(Received 18 April 2007; accepted 29 August 2007; published online 26 October 2007)

It is noted that in large eddy simulation (LES), filtering of the three-point third-order velocity correlation allows one to determine the two-point third-order correlation of the filtered velocity. This is useful in analyzing the dynamics of filtered (LES) fields, since the two-point third-order correlation describes energy flux from large to small scales, just as it does in unfiltered turbulence. A model for the three-point third-order correlation for stationary, incompressible, homogeneous, isotropic turbulence in the inertial range is proposed in which simple polynomials are used as the scalar function appearing in the most general tensorial form for the correlation. This leads to a model with four free parameters, which are set by appealing to statistical data from a direct numerical simulation. The resulting three-point third-order correlation function is in very good agreement with the data. © *2007 American Institute of Physics*. [DOI: 10.1063/1.2793163]

I. INTRODUCTION

Multipoint velocity correlations are central to the statistical description of homogeneous isotropic turbulence.[1,2] The two-point second-order velocity correlation $\mathbb{R}_{ij}(\mathbf{r}) = \langle v_i(\mathbf{x}) v_j(\mathbf{x}+\mathbf{r}) \rangle$, and its Fourier transform, the spectrum tensor, are among the most commonly considered correlations, and a variety of models for their evolution have been developed.[3–6] There have also been a number of theoretical and experimental efforts to analyze two-point correlations and structure functions,[7,8] including applications to large eddy simulation modeling.[9]

In homogeneous turbulence, the evolution equation for $\mathbb{R}$ contains the two-point third-order correlation $\mathbb{S}_{ijk}(\mathbf{r}) = \langle v_i(\mathbf{x}) v_j(\mathbf{x}) v_k(\mathbf{x}+\mathbf{r}) \rangle$ as a result of the nonlinear terms in the Navier–Stokes equations. $\mathbb{S}$ describes the transfer of energy from large-scales to small, and as such is of critical importance to the theory of the two-point statistics of turbulence. Assuming isotropy, the evolution equation for $\mathbb{R}$ reduces to the von Karman–Howarth equation.[10] In combination with the assumption of a Kolmogorov inertial range, this leads to the well-known Kolmogorov 4/5 law[11] for the third-order longitudinal structure function in the inertial range. This is an exact consequence of scale separation between large and dissipative scales and the scale independence of the energy flux in the intermediate range between them for homogeneous, isotropic, incompressible turbulence. Isotropy of the turbulence also implies that $\mathbb{S}$ can be uniquely determined in terms of the third-order structure function, just as $\mathbb{R}$ can be written in terms of the second-order structure function.

Of course, the two-point third-order correlation $\mathbb{S}_{ijk}(\mathbf{r})$ is a restricted case of the three-point third-order correlation $\mathbb{T}_{ijk}(\mathbf{r},\mathbf{s}) = \langle v_i(\mathbf{x}) v_j(\mathbf{x}+\mathbf{r}) v_k(\mathbf{x}+\mathbf{s}) \rangle$. But there is no direct association of $\mathbb{T}$ with the evolution equation for $\mathbb{R}$ or with energy transfer. There has thus been little motivation to study $\mathbb{T}$, and because of the complexity of this quantity, there has been virtually no work to characterize it.

In large eddy simulation (LES), however, there is a motivation to characterize $\mathbb{T}$. To see why this is true, let $\tilde{v}_i(\mathbf{x})$ be the LES filtered velocity field. Note that the evolution equation for the two-point correlation of a LES field $\tilde{\mathbb{R}}_{ij}(\mathbf{r}) = \langle \tilde{v}_i(\mathbf{x}) \tilde{v}_j(\mathbf{x}+\mathbf{r}) \rangle$ includes a term involving the two-point third-order correlation of the LES field $\tilde{\mathbb{S}}_{ijk}(\mathbf{r}) = \langle \tilde{v}_i(\mathbf{x}) \tilde{v}_j(\mathbf{x}) \tilde{v}_k(\mathbf{x}+\mathbf{r}) \rangle$, that arises from the quadratic terms in the LES equations. $\tilde{\mathbb{S}}$ represents energy transfer among scales in the LES due to the nonlinear term and is thus of importance in analyzing the dynamics of the LES equations. It is also one of the statistical inputs to the optimal LES modeling approach described in Refs. 12–14. $\tilde{\mathbb{S}}$ can be determined by applying the filter (three times) to $\mathbb{T}$ (see Sec. II A), which is the reason for our interest in the three-point correlation.

The notable exception to the lack of work on the three-point third-order correlation is the paper by Proudman and Reid,[15] in which the most general incompressible, isotropic form of the Fourier transform of $\mathbb{T}$ is derived. In this paper, we start with some mathematical background (Sec. II). Then from Proudman and Reid's result for the Fourier transform of the correlation, the equivalent form for the physical-space correlation is determined and we find the simplest expression consistent with the Kolmogorov 4/5 law (Sec. III). Conclusions and implications are discussed in Sec. IV.

II. BACKGROUND

The Kolmogorov inertial range theory for high Reynolds number turbulence yields expressions for the longitudinal structure functions, under the well known similarity assumptions that in the inertial range, the statistical properties of turbulence depend on the separation scale and the rate of dissipation.[1,16] The longitudinal structure functions are

$$S_p(r) = \langle (u_\parallel(\mathbf{x}+\mathbf{r}) - u_\parallel(\mathbf{x}))^p \rangle = C_p(\epsilon r)^{p/3}, \tag{1}$$

where $r=|\mathbf{r}|$ is the magnitude of the separation vector $\mathbf{r}$, which is assumed to be in the inertial range, $u_\parallel$ is the velocity component in the separation direction, ϵ is the average rate of kinetic energy dissipation (per unit mass), and C_p are the Kolmogorov constants, which are generally determined empirically (e.g., $C_2 \approx 2.0$). The Kolmogorov expressions for the structure functions are found to be relatively good representations for $p=2$ and 3, though corrections are available for $p=2$.[17,18] However, their accuracy degrades as p increases.[19] Remarkably, an exact consequences of the theory and the evolution equation for the two-point correlation, in which the third-order two-point correlation appears, is that $C_3=-4/5$, the so-called Kolmogorov 4/5 law.

Isotropy and the continuity constraints are sufficient to determine the second- and third-order two-point correlation tensors from the second and third-order structure functions, respectively. Using the Kolmogorov expressions above, the correlation tensors are

$$\mathbb{R}_{ij}(\mathbf{r}) = u^2 \delta_{ij} + \frac{C_2}{6}(\epsilon r)^{2/3}\left(\frac{r_i r_j}{r^2} - 4\delta_{ij}\right), \tag{2}$$

$$\mathbb{S}_{ijk}(\mathbf{r}) = \frac{\epsilon}{15}\left(\delta_{ij} r_k - \frac{3}{2}(\delta_{ik} r_j + \delta_{jk} r_i)\right), \tag{3}$$

where the two-point correlations are defined as

$$\mathbb{R}_{ij}(\mathbf{r}) = \langle v_i(\mathbf{x}) v_j(\mathbf{x}+\mathbf{r}) \rangle, \tag{4}$$

$$\mathbb{S}_{ijk}(\mathbf{r}) = \langle v_i(\mathbf{x}) v_j(\mathbf{x}) v_k(\mathbf{x}+\mathbf{r}) \rangle, \tag{5}$$

and u^2 is 2/3 the turbulent kinetic energy, which is also the velocity variance. The result for the second-order correlation is well known, but we are not aware of a previous reporting of the third-order two-point correlation as shown here, though it is implicit to the derivation of the 4/5 law, and is alluded to by Frisch.[1] For completeness, an outline of the derivation is given in Appendix A.

The three-point third-order velocity correlation, which is the quantity of interest here is defined as

$$\mathbb{T}_{ijk}(\mathbf{r},\mathbf{s}) = \langle v_i(\mathbf{x}) v_j(\mathbf{x}+\mathbf{r}) v_k(\mathbf{x}+\mathbf{s}) \rangle. \tag{6}$$

The three points form a triangle, and vectors $\mathbf{r}$ and $\mathbf{s}$ determine its size, shape, and orientation. Because it is a function of two vector arguments, $\mathbb{T}$ is much more complex than the two-point correlation $\mathbb{S}$. However, we seek the analog of Eq. (3) for the three-point correlation. That is a "simple" tensor form consistent with known constraints and the Kolmogorov theory, particularly the 4/5 law.

A. Relationship to LES

In the usual formulation of LES the filtered velocity is defined as

$$\tilde{v}_i(\mathbf{x}) = \int G(\mathbf{x}-\mathbf{x}') v_i(\mathbf{x}') d\mathbf{x}', \tag{7}$$

where $G(\mathbf{x})$ is the homogeneous filter kernel. The Navier–Stokes equations are then filtered to arrive at an evolution equation for $\tilde{\mathbf{v}}$,

$$\frac{\partial \tilde{v}_i}{\partial t} + \frac{\partial \tilde{v}_i \tilde{v}_j}{\partial x_j} = -\frac{1}{\rho}\frac{\partial \tilde{P}}{\partial x_i} + \nu \frac{\partial^2 \tilde{v}_i}{\partial x_j \partial x_j} + \frac{\partial \tau_{ij}}{\partial x_j}, \tag{8}$$

where

$$\tau_{ij} = \tilde{v}_i \tilde{v}_j - \widetilde{v_i v_j} \tag{9}$$

is the subgrid stress.

In homogeneous, isotropic, incompressible turbulence, the two-point correlation of the filtered velocity $\tilde{\mathbb{R}}_{ij}(\mathbf{r}) = \langle \tilde{v}_i(\mathbf{x}) \tilde{v}_j(\mathbf{x}+\mathbf{r}) \rangle$ evolves according to

$$\frac{\partial \tilde{\mathbb{R}}_{ik}}{\partial t} = 2\nu \frac{\partial^2 \tilde{\mathbb{R}}_{ik}}{\partial r_j \partial r_j} + \frac{\partial \tilde{\mathbb{S}}_{ijk}}{\partial r_j} + \frac{\partial \tilde{\mathbb{S}}_{kji}}{\partial r_j} - \frac{\partial \mathbb{Q}_{ijk}}{\partial r_j} - \frac{\partial \mathbb{Q}_{kji}}{\partial r_j}, \tag{10}$$

where

$$\tilde{\mathbb{S}}_{ijk}(\mathbf{r}) = \langle \tilde{v}_i(\mathbf{x}) \tilde{v}_j(\mathbf{x}) \tilde{v}_k(\mathbf{x}+\mathbf{r}) \rangle, \tag{11}$$

$$\mathbb{Q}_{ijk}(\mathbf{r}) = \langle \tau_{ij}(\mathbf{x}) \tilde{v}_k(\mathbf{x}+\mathbf{r}) \rangle. \tag{12}$$

The energy transfer between scales of the filtered velocity is mediated by $\tilde{\mathbb{S}}$. We can contract Eq. (10) to obtain the evolution equation for $\frac{1}{2}\tilde{\mathbb{R}}_{ii}$, which only depends on the magnitude of $\mathbf{r}$, and can be interpreted as the energy in the filtered field associated with scales larger than r. Then $-\partial \tilde{S}_{iji}/\partial r_j(r)$ appears as the net flux of energy from scales larger than r in the filtered field to those smaller than r. This is analogous to the physical-space energy flux $-\partial S_{iji}/\partial r_j$ in the unfiltered equation,[1] which is just ϵ in the inertial range. Similarly $\partial \mathbb{Q}_{iji}/\partial r_j$ is interpreted as the net flux of energy from scales of the filtered fields larger than r to the subfilter fluctuations $(\mathbf{v}-\tilde{\mathbf{v}})$. These average fluxes are generally positive (from large to small scales); but this is an average of fluxes in both directions.

Because $\tilde{\mathbb{S}}$ includes the product of filtered velocities, it cannot be determined by directly filtering $\mathbb{S}$. It can, however be found by filtering $\mathbb{T}$,

$$\tilde{\mathbb{S}}_{ijk}(\mathbf{r}) = \int\int\int G(\mathbf{s}) G(\mathbf{s}-\mathbf{r}') G(\mathbf{s}+\mathbf{r}-\mathbf{s}') \times \mathbb{T}_{ijk}(\mathbf{r}',\mathbf{s}') d\mathbf{s} d\mathbf{r}' d\mathbf{s}' \tag{13}$$

which can be derived easily by applying the filter (7) separately to each of the velocities in the definition of $\mathbb{T}$.

The two-point correlation Eq. (10) also includes $\mathbb{Q}$ arising from the subfilter stress term in the LES equations. The definition of τ_{ij} (9) means that $\mathbb{Q}$ can be expressed as

$$\mathbb{Q}_{ijk}(\mathbf{r}) = \widetilde{\mathbb{S}}_{ijk}(\mathbf{r}) - \hat{\mathbb{S}}_{ijk}(\mathbf{r}), \tag{14}$$

where $\hat{\mathbb{S}}_{ijk}(\mathbf{r}) = \widetilde{\langle v_i v_j(\mathbf{x}) \tilde{v}_k(\mathbf{x}+\mathbf{r})\rangle}$ can be determined by filtering the two-point third-order correlation of the unfiltered velocity

$$\hat{\mathbb{S}}_{ijk}(\mathbf{r}) = \int\int G(\mathbf{s}) G(\mathbf{s}+\mathbf{r}-\mathbf{r}') \mathbb{S}_{ijk}(\mathbf{r}') d\mathbf{s} d\mathbf{r}'. \tag{15}$$

Thus for the purpose of analyzing LES, we are motivated to develop a model for the three-point third-order correlation tensor. This will allow us to determine contributions of both the nonlinear terms and the subfilter stress to energy dynamics.

B. The Fourier transform of $\mathbb{T}$

Proudman and Reid[15] determined a general form for the Fourier transform of $\mathbb{T}$ in both $\mathbf{r}$ and $\mathbf{s}$ (this is a six-dimensional Fourier transform). For an incompressible, homogeneous, isotropic turbulence, the most general possible form for the Fourier transform Φ of $\mathbb{T}$ is given by

$$\Phi_{ijk}(\boldsymbol{\rho},\boldsymbol{\sigma}) = \Delta_{im}(\boldsymbol{\tau})\Delta_{jn}(\boldsymbol{\rho})\Delta_{kp}(\boldsymbol{\sigma})[\delta_{np}\rho_m\phi + \delta_{mp}\sigma_n\phi_1 + \delta_{mn}\rho_p\phi_2 + \rho_m\sigma_n\rho_p\zeta], \tag{16}$$

where the wavevectors $\boldsymbol{\rho}$, $\boldsymbol{\sigma}$, and $\boldsymbol{\tau}$ are interrelated $\boldsymbol{\rho}+\boldsymbol{\sigma}+\boldsymbol{\tau}=0$, and $\Delta_{im}(\boldsymbol{\rho}) = \delta_{im} - \rho_i\rho_m/\rho^2$ is the divergence-free projector. The scalar functions ϕ, ϕ_1, ϕ_2, and ζ depend only on the magnitudes of the wavevectors. For an outline of the derivation of Eq. (16), see Appendix B. Symmetries in the tensor $\mathbb{T}$ imply symmetries among scalar functions

$$\phi(\rho,\sigma,\tau) = -\phi(\sigma,\rho,\tau) = \phi_1(\tau,\rho,\sigma) = \phi_2(\rho,\tau,\sigma). \tag{17}$$

Proudman and Reid[15] also analyze the dynamic equation for Φ in the context of the quasinormal approximation to find independent (model) dynamic equations for ϕ and ζ. These equations imply that for stationary turbulence, ζ is zero. We will thus assume that $\zeta=0$, and with the symmetries expressed in Eq. (17), Φ is determined through Eq. (16) by a single scalar function ϕ of ρ, σ, and τ. We start with this form in developing our real-space model for $\mathbb{T}$.

III. INERTIAL-RANGE MODEL OF $\mathbb{T}$

To construct a model for the three-point third-order correlation, a general tensor form consistent with Eq. (16) is derived, and then the scalar function appearing in the expression is selected for consistency with the Kolmogorov 4/5 law.

A. A general form for $\mathbb{T}$ in real space

To develop the analog of Eq. (16) in real space, it will be inverse Fourier transformed to yield an expression for $\mathbb{T}$. However, to simplify the computations in real-space, it is convenient to recast the expression as

$$\Phi_{ijk}(\boldsymbol{\rho},\boldsymbol{\sigma}) = \tilde{\Delta}_{im}(\boldsymbol{\tau})\tilde{\Delta}_{jn}(\boldsymbol{\rho})\tilde{\Delta}_{kp}(\boldsymbol{\sigma})[\delta_{np} i\rho_m \tilde{\phi}(\rho,\sigma,\tau) + \delta_{mp} i\sigma_n \tilde{\phi}(\sigma,\tau,\rho) + \delta_{mn} i\rho_p \tilde{\phi}(\rho,\tau,\sigma)], \tag{18}$$

where $\tilde{\Delta}_{im}(\boldsymbol{\rho}) = \rho^2\delta_{im} - \rho_i\rho_m$ is a modified divergence free operator, and $\tilde{\phi}(\rho,\sigma,\tau) = -i\phi(\rho,\sigma,\tau)/(\rho\sigma\tau)^2$ is a modified scalar function that has the same symmetry properties as ϕ. The advantage of this form is that the inverse Fourier transform will not give rise to inverse Laplacian operators. An inverse Fourier transform of Eq. (18) yields

$$\mathbb{T}_{ijk}(\mathbf{r},\mathbf{s}) = \mathcal{P}^t_{im}\mathcal{P}^s_{jn}\mathcal{P}^r_{kp}[\delta_{np}\partial^s_m\psi(r,s,t) + \delta_{mp}\partial^r_n\psi(t,r,s) + \delta_{mn}\partial^s_p\psi(t,s,r)] \tag{19}$$

which is thus our general expression for $\mathbb{T}$ in stationary, homogeneous, isotropic incompressible turbulence. Here, the third separation vector is $\mathbf{t}=\mathbf{r}-\mathbf{s}$, the scalar function $\psi(r,s,t)$ is the inverse Fourier transform of $\tilde{\phi}$, and r, s, and t are the magnitudes of the separation vectors $\mathbf{r}$, $\mathbf{s}$, and $\mathbf{t}$, respectively. The operators appearing in Eq. (19) are defined as

$$\partial^r_i \equiv \left.\frac{\partial}{\partial s_i}\right|_{\mathbf{r}}, \tag{20}$$

$$\partial^s_i \equiv \left.\frac{\partial}{\partial r_i}\right|_{\mathbf{s}}, \tag{21}$$

$$\partial^t_i \equiv -\left.\frac{\partial}{\partial r_i}\right|_{\mathbf{s}} - \left.\frac{\partial}{\partial s_i}\right|_{\mathbf{r}}, \tag{22}$$

$$\mathcal{P}^\alpha_{ij} \equiv \delta_{ij}\partial^\alpha_k\partial^\alpha_k - \partial^\alpha_i\partial^\alpha_j. \tag{23}$$

It is straightforward to confirm that the expression for $\mathbb{T}$ in Eq. (19) satisfies the relevant symmetry and continuity constraints for the third-order three-point correlation, provided that

$$\psi(r,s,t) = -\psi(s,r,t), \tag{24}$$

which is the analog of Eq. (17). The constraints on $\mathbb{T}$ are

$$\partial^t_i \mathbb{T}_{ijk} = \partial^s_j \mathbb{T}_{ijk} = \partial^r_k \mathbb{T}_{ijk} = 0, \tag{25}$$

$$\mathbb{T}_{ijk}(\mathbf{r},\mathbf{s}) = \mathbb{T}_{ikj}(\mathbf{s},\mathbf{r}), \tag{26}$$

$$\mathbb{T}_{ijk}(\mathbf{r},\mathbf{s}) = \mathbb{T}_{jki}(-\mathbf{t},-\mathbf{r}), \tag{27}$$

$$\mathbb{T}_{ijk}(\mathbf{r},\mathbf{s}) = \mathbb{T}_{kij}(-\mathbf{s},\mathbf{t}). \tag{28}$$

The tensor form given in Eq. (19) is clearly linear in ψ; indeed it can be expressed as

$$\mathbb{T}_{ijk} = \mathcal{L}_{ijk}(\psi), \tag{29}$$

where $\mathcal{L}_{ijk}$ is the tensor-valued linear operator implied by Eq. (19). To complete the model of the three-point third-order correlation, we need to only specify $\psi(r,s,t)$ satisfying Eq. (24).

B. Scalar function ψ in the inertial range

Our primary interest is a model for $\mathbb{T}$ that is valid in the inertial range, analogous to the inertial range expression for $\mathbb{S}$ (3). Kolmogorov's 4/5 law constrains $\mathbb{S}$ to vary linearly with separation. Since $\mathbb{T}$ must reduce to $\mathbb{S}$ when r, s or t are zero, this linearity must be reflected in $\mathbb{T}$ as well. More generally, the Kolmogorov similarity argument[1,11] requires that in the inertial range

$$\mathbb{T}(\alpha\mathbf{r},\alpha\mathbf{s}) = \alpha\mathbb{T}(\mathbf{r},\mathbf{s}). \tag{30}$$

The simplest way to ensure this linearity is to choose $\psi(r,s,t)$ to be a polynomial in r, s, and t. Since each term in Eq. (19) is a seventh derivative of ψ, only terms with a total degree of 8, will contribute to the linear scaling of $\mathbb{T}$. This, along with the symmetry constraint on ψ (24) suggests that ψ be constructed from terms of the form

$$p_{a,b} \equiv (r^a s^b - r^b s^a)t^c \tag{31}$$

with $a+b+c=8$ and a, b, $c \geq 0$. There are only 20 expressions of this form, and of these 14 produce nonzero $\mathbb{T}$ when substituting for ψ in Eq. (19).

However, all of these 14 nontrivial $\mathbb{T}$ are singular when r, s, or t are zero. For example, terms such as $r_i r_j r_k r/s^3$ arise, which is clearly singular at $s=0$. In addition, terms like $\delta_{ij}s_k r/s$ arise, which is discontinuous at $s=0$. It was found, however, that there is a five-dimensional null space of the singular and discontinuous terms. There is thus a five-dimensional space of possible ψ functions that yield nonsingular, continuous $\mathbb{T}$. The space is spanned by the following five functions:

$$\psi^1 = \tfrac{1}{5760}[-27p_{0,3} - 3p_{0,5} + 4p_{2,3} + 18p_{3,5}], \tag{32}$$

$$\psi^2 = \tfrac{1}{1155840}[-315p_{0,3} + 4p_{0,7} + 56p_{2,5} - 140p_{3,4} + 1260p_{3,5}], \tag{33}$$

$$\psi^3 = \tfrac{1}{1257600}[-4p_{0,1} - 1935p_{0,3} - 40p_{1,2} + 80p_{1,3} - 60p_{1,4} + 16p_{1,5} + 180p_{2,3} + 990p_{3,5}], \tag{34}$$

$$\psi^4 = \tfrac{1}{462720}[-4p_{0,1} - 1215p_{0,3} - 36p_{1,2} + 64p_{1,3} - 36p_{1,4} + 4p_{1,6} + 108p_{2,3} - 20p_{2,5} + 40p_{3,4} + 270p_{3,5}], \tag{35}$$

$$\psi^5 = \tfrac{1}{10684800}[-60p_{0,1} - 16065p_{0,3} - 504p_{1,2} + 840p_{1,3} - 420p_{1,4} + 24p_{1,7} + 1260p_{2,3} + 7560p_{3,5}], \tag{36}$$

where $p_{i,j}$ are as defined in Eq. (31) above. These functions have been normalized so that each of the $\mathbb{T}^n = \mathcal{L}(\psi^n)$ satisfies

$$\mathbb{T}^n_{ijk}(0,\mathbf{r}) = \tfrac{1}{15}\left[\delta_{ij}r_k - \tfrac{3}{2}(\delta_{ik}r_j + \delta_{jk}r_i)\right] \tag{37}$$

which is just Eq. (3) with ϵ set to 1. The analytic model we seek for $\mathbb{T}$ is thus given by

$$\mathbb{T}_{ijk}(\mathbf{r},\mathbf{s}) = \sum_{n=1}^{5} a_n \mathbb{T}^n_{ijk}(\mathbf{r},\mathbf{s}) \quad \text{with} \sum_{n=1}^{5} a_n = \epsilon. \tag{38}$$

While the scalar basis functions ψ^n are relatively simple to write down, Eqs. (32)–(36), the basis tensors $\mathbb{T}^n$ are not. Indeed the expressions are so complex (as many as 758 terms), that they will not be written out here. The process by which the calculations were performed is described in Appendix C and programs are available through EPAPS[20] and at http://turbulence.ices.utexas.edu to evaluate the tensor numerically.

To display the features of the five basis tensors defined above, we examine the various components of the tensor for two special arrangements of the separation vectors. First is with the separation vectors $\mathbf{r}$ and $\mathbf{s}$ collinear (parallel, designated by $\parallel$), which, without loss of generality, we choose to be in the x_1 direction ($\mathbf{r}=r\mathbf{e}_1, \mathbf{s}=s\mathbf{e}_1$). In this case, there are only seven nonzero components, of which only $\mathbb{T}^{\parallel}_{111}$ and $\mathbb{T}^{\parallel}_{122}$ are independent. The other five ($\mathbb{T}^{\parallel}_{212}$, $\mathbb{T}^{\parallel}_{221}$, $\mathbb{T}^{\parallel}_{133}$, $\mathbb{T}^{\parallel}_{313}$, and $\mathbb{T}^{\parallel}_{331}$) are related to $\mathbb{T}^{\parallel}_{122}$ through symmetry.

The second separation vector configuration is with $\mathbf{r}$ and $\mathbf{s}$ orthogonal (designated by $\perp$). Again, without loss of generality $\mathbf{r}=r\mathbf{e}_1$ is chosen to be in the x_1-direction, and $\mathbf{s}=s\mathbf{e}_2$ is chosen in the x_2-direction. In this configuration, there are 14 nonzero components, of which seven are independent: $\mathbb{T}^{\perp}_{111}$, $\mathbb{T}^{\perp}_{112}$, $\mathbb{T}^{\perp}_{121}$, $\mathbb{T}^{\perp}_{122}$, $\mathbb{T}^{\perp}_{133}$, $\mathbb{T}^{\perp}_{313}$, and $\mathbb{T}^{\perp}_{323}$. Each of these is one of a pair of symmetrically related components.

Since the tensor functions vary linearly with separation, the tensors can be normalized by $q \equiv \max(r,s,t)$, which for the special separation configurations considered leaves only the dependence on s/r. The nonzero, nonredundant components of $\mathbb{T}^{\parallel}/q$ and $\mathbb{T}^{\perp}/q$ are shown in Fig. 1 as a function of $\theta = \arctan(s/r)$. Note that the five basis tensors have similar structure, and that two of them are quite similar ($\mathbb{T}^3 = \times$ and $\mathbb{T}^5 = \square$). There has been no effort to orthogonalize the basis.

C. Fitting to DNS data

To determine the five coefficients $\{a_1, a_2, \ldots, a_5\}$ in Eq. (38), a least-squares fit to data from a direct numerical simulation (DNS) of forced isotropic turbulence at $\mathrm{Re}_\lambda = 164$,[12] is performed. Let $\mathbb{E}(\mathbf{r},\mathbf{s}) = \mathbb{T}^{\mathrm{DNS}} - \mathbb{T}^{\mathrm{model}}$, be the error tensor. Then the fitting was done to minimize the objective function

$$F = \left(1 - \frac{2}{\pi}\right) \int \mathbb{E}^{\parallel}_{ijk}(r,s)\mathbb{E}^{\parallel}_{ijk}(r,s)drds + \frac{2}{\pi}\int \mathbb{E}^{\perp}_{ijk}(r,s)\mathbb{E}^{\perp}_{ijk}(r,s)drds \tag{39}$$

under the constraint that $\Sigma_n a_n = \epsilon$, where only separation vectors $\mathbf{r}$ and $\mathbf{s}$ that are parallel or perpendicular are considered, to reduce the data requirements to a manageable level, and the integrals are taken over the domain in r and s for which q is in the approximate inertial range for the DNS ($q/\lambda \in [0.72, 1.2]$) or ($q/\eta \in [19, 32]$). This objective was selected as a (crude) approximation to the integral over all $\mathbf{r}$ and $\mathbf{s}$ in the inertial range. The coefficients obtained from this fit are given in Table I. The coefficient of determination

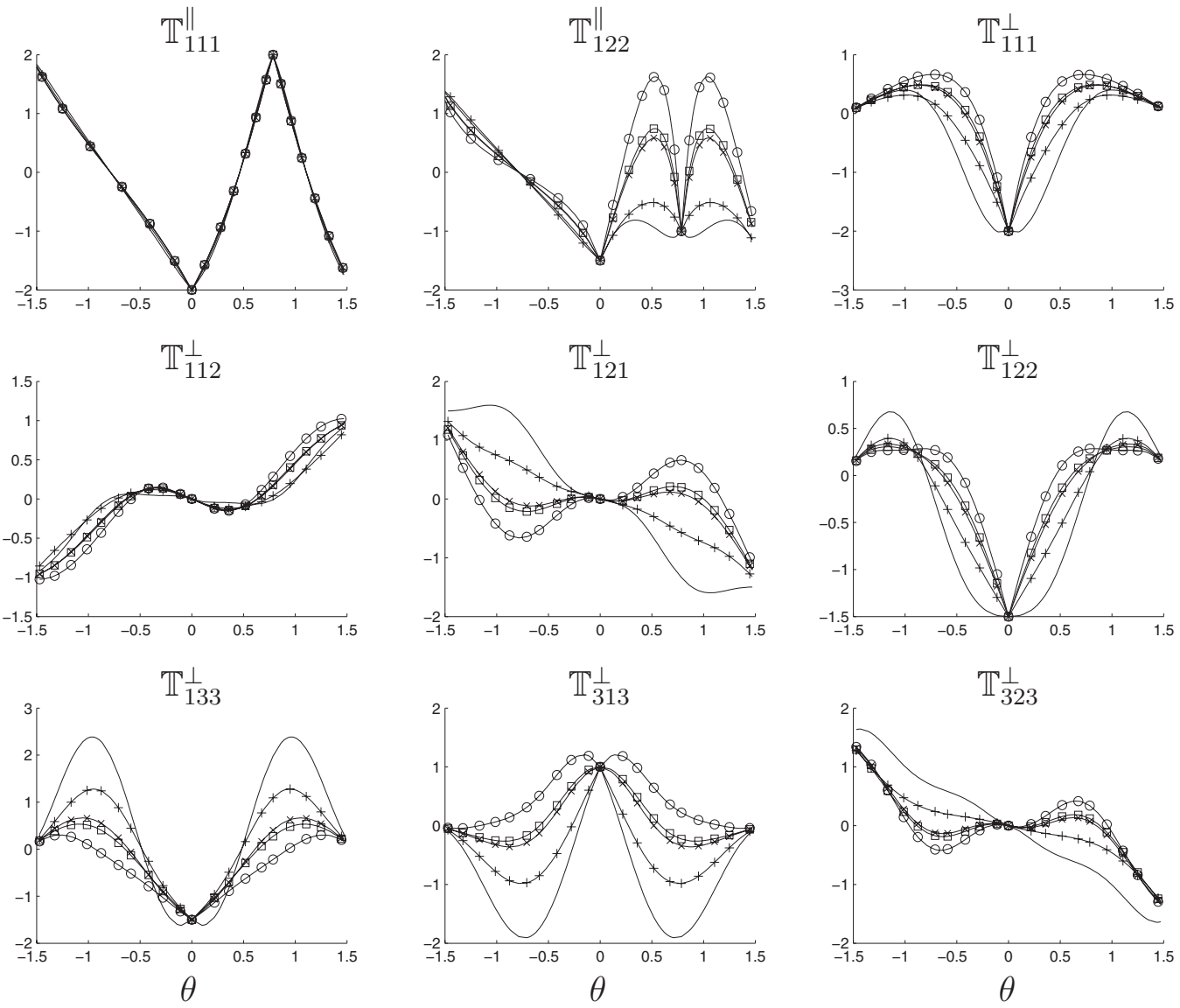

FIG. 1. Basis functions for the nonzero, nonredundant components of $\mathbb{T}^{\parallel}/q$ and $\mathbb{T}^{\perp}/q$ (see text for definitions) as functions of $\theta=\arctan(s/r)$. $\mathbb{T}^1$=(plain curve), $\mathbb{T}^2$=+, $\mathbb{T}^3$=×, $\mathbb{T}^4$=○, and $\mathbb{T}^5$=□.

is $R^2=0.96$, indicating that our model describes the DNS data quite well.

The ability of the model to represent the DNS correlations is shown in Fig. 2, in which nonzero components of $\mathbb{T}/q$ are plotted as a function of θ, for the parallel and perpendicular separation vectors, as in Fig. 1. The agreement between model and DNS is very good. One exception is the discrepancy in $\mathbb{T}^{\perp}_{111}$. This may be a problem with the DNS data rather than the model, because the DNS data were significantly unsymmetric which implies a lack of statistical convergence in the DNS data for this component. Further indication of the quality of the model is given in Fig. 3, where contour plots show the nonzero components of $\mathbb{T}$ as functions of r and s in both the model and the DNS. Since there is a symmetry in each term shown, the DNS and model are shown together in each frame, with a line of symmetry dividing them. The model and DNS are very similar. But, there is a minor discrepancy for r and s near zero, which is due to viscous effects not represented in the model.

TABLE I. Values of the model coefficients in Eq. (38) found by fitting the DNS data of Langford and Moser (Ref. 12).

a_1/ϵ	0.884
a_2/ϵ	−2.692
a_3/ϵ	−6.099
a_4/ϵ	−5.853
a_5/ϵ	14.760

IV. DISCUSSION AND IMPLICATIONS

It is remarkable that the simple considerations of isotropy and the Kolmogorov similarity assumptions are sufficient to exactly determine the two-point third-order correlation $\mathbb{S}$, a third-ranked tensor. The three-point third-order correlation $\mathbb{T}$ is a much more complicated object, so it is equally remarkable that the same considerations, along with a plausible modeling ansatz regarding functional forms (31), is sufficient to specify a model for $\mathbb{T}$ in the inertial range

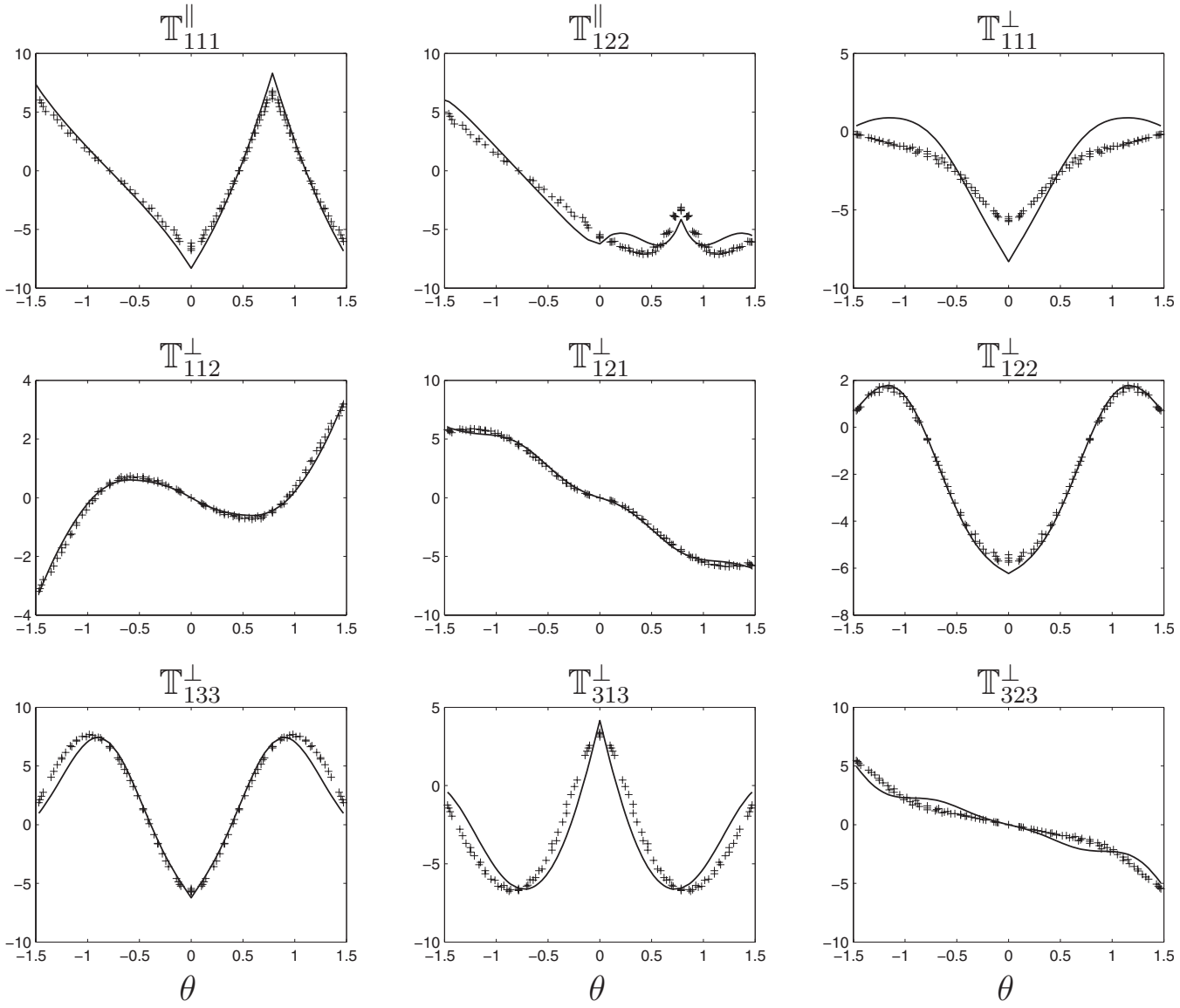

FIG. 2. The nonzero, nonredundant components of $\mathbb{T}^{\parallel}/q$ and $\mathbb{T}^{\perp}/q$ (see text for definitions) as functions of $\theta=\arctan(s/r)$ from the DNS data of Ref. 12 (crosses) and the tensor model given by Eq. (38) and Table I (curve).

with just four free constants. The model appears to fit low Reynolds number DNS data quite well. It would also be useful to test the model against higher Reynolds number DNS data.

While the considerations leading to the model are simple, the model itself is algebraically very complex. A special-purpose tensor algebra program was written to perform the necessary manipulations. The detailed results are available through EPAPS[20] and at http://turbulence.ices.utexas.edu, as are programs used to evaluate the tensors numerically. Given the complexity of the expressions, it may be that the ability to evaluate tensor components numerically will be most useful.

The three-point third-order correlation $\mathbb{T}$ is of particular interest in the analysis and modeling of LES, because by applying the LES filter to $\mathbb{T}$ one can determine third-order correlations of the filtered velocity. This is important in analyzing the transfer of energy among scales, and in formulating LES models. For example, the representation of $\mathbb{T}$ will allow optimal LES models[12] of the type evaluated by Zandonade *et al.*[13] to be formulated theoretically, the usefulness of such a model will have to be evaluated *a posteriori* by validation of simulations performed with the model.

As another example of the utility of the correlation in analyzing the impact of filtering, $\mathbb{T}$ was used to evaluate the third-order longitudinal structure function of the filtered velocity by using Eq. (13) to evaluate $\widetilde{S}_3(r)=6\widetilde{\mathbb{S}}_{111}(r\mathbf{e}_1)$ for a Gaussian filter kernel given by

$$G(\mathbf{x}) = \frac{1}{\Delta\sqrt{2\pi}} e^{-|\mathbf{x}|^2/2\Delta^2}, \tag{40}$$

where Δ is the filter width. The result is plotted in Fig. 4 along with S_3 given by the 4/5 law. This filter is isotropic so it preserves the isotropy of the filtered field, implying that $\widetilde{\mathbb{S}}_{ijk}$ is written in terms of $\widetilde{S}_3$ in the same way that $\mathbb{S}_{ijk}$ is determined from S_3 (see Appendix A). Furthermore, the filter is homogeneous and $\partial\mathbb{S}_{ijk}/\partial r_j$ is a constant in the inertial range, so Eq. (15) gives

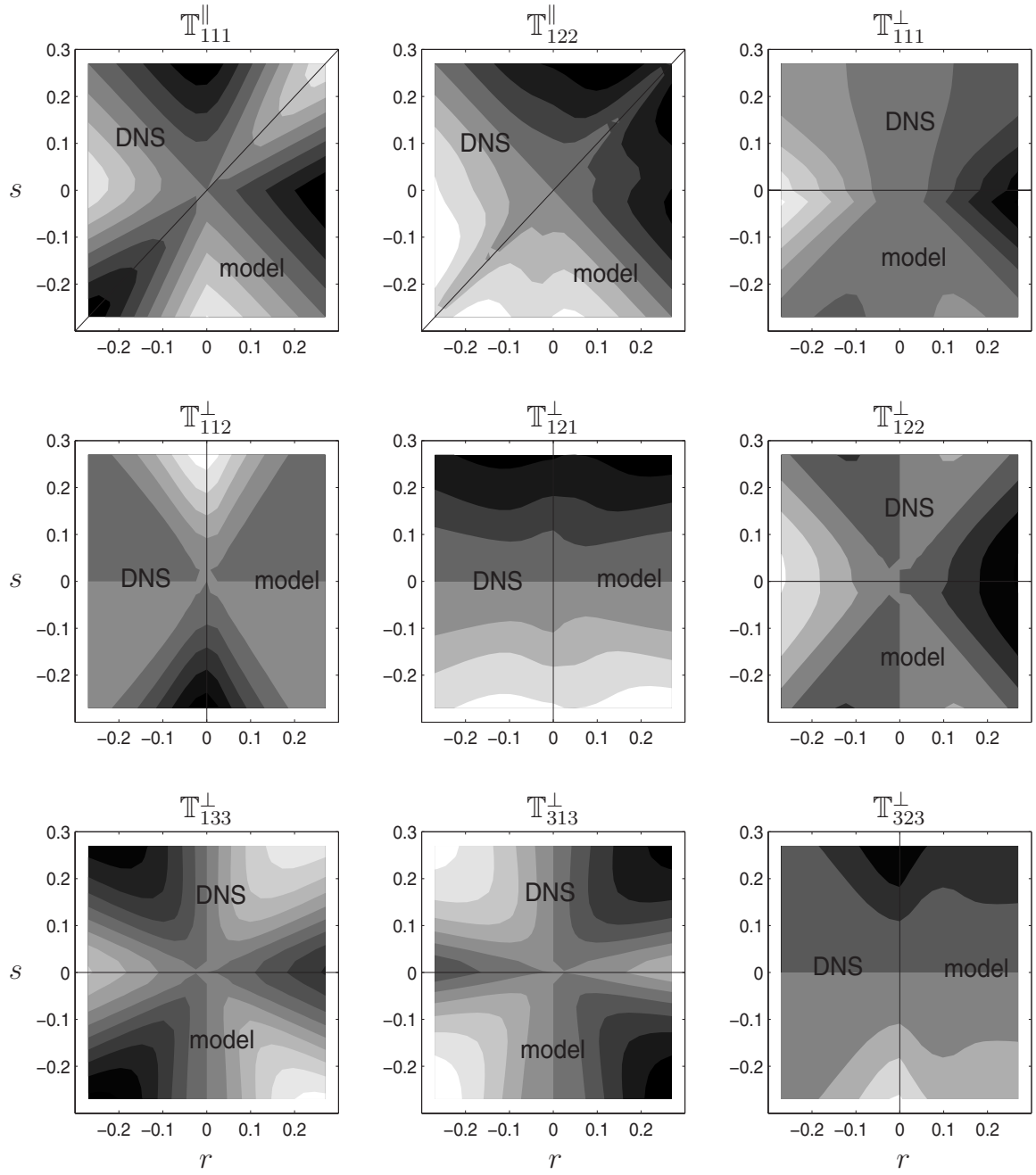

FIG. 3. Contours of the DNS data of Ref. 12 and the tensor model given by Eq. (38) and Table I for $\mathbb{T}^{\parallel}$ and $\mathbb{T}^{\perp}$ (see text for definitions) in the r-s plane. Each component has a symmetry, which is used to allow the data and the model to be displayed side-by-side, as shown. The heavy black lines are lines of symmetry for each component.

$$\frac{\partial \hat{\mathbb{S}}_{ijk}}{\partial r_j} = \frac{\partial \mathbb{S}_{ijk}}{\partial r_j} = -\frac{\epsilon}{3}\delta_{ik}. \tag{41}$$

Therefore, $\mathbb{Q}$ (14) is directly determined from the difference between S_3 and $\widetilde{S}_3$ shown in Fig. 4. In particular, using Eq. (A3) we can write the energy fluxes $\partial \widetilde{\mathbb{S}}_{iji}/\partial r_j = F(\widetilde{S}_3)$ and $\partial \widetilde{\mathbb{Q}}_{iji}/\partial r_j = F(\widetilde{S}_3 - S_3)$, where the operator F is given by

$$F[S(r)] = \frac{2}{3r}S + \frac{7}{12}\frac{dS}{dr} + \frac{r}{12}\frac{d^2S}{dr^2}. \tag{42}$$

These two energy fluxes are also shown in Fig. 5. It is interesting that the flux to the subfilter scales goes to zero so slowly with increasing r, only reaching 10% of the dissipation by $r=15\Delta$. Further, because $\widetilde{S}_3 - S_3$ goes to a constant for large r, the subfilter flux only goes to zero like $1/r$.

ACKNOWLEDGMENTS

The authors would like to thank Dr. Amitabh Bhattacharya, who helped with the analysis, and Dr. Paulo Zandonade, who provided the DNS data. The support of the National Science Foundation (CTS-0352552) and Air Force Office of Scientific Research (F49620-04-1-0032) is gratefully acknowledged.

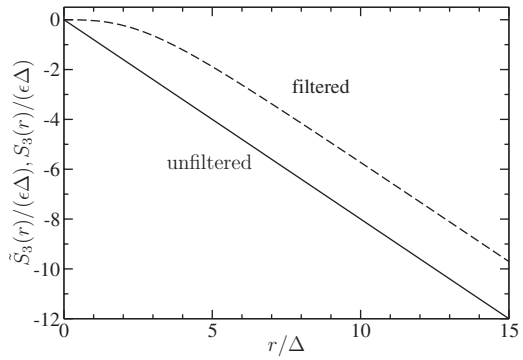

FIG. 4. Third-order longitudinal structure function $\tilde{S}_3$ of a Gaussian filtered infinite Reynolds number isotropic turbulence computed from the tensor model described by Eq. (38) and Table I. Also shown is the unfiltered structure function S_3 from the Kolmogorov 4/5 law.

APPENDIX A: DETERMINATION OF $\mathbb{S}$ IN THE INERTIAL RANGE

The derivation of Eq. (3) starts from the general form of an isotropic third-rank tensor function of a vector argument,

$$\mathbb{S}_{ijk}(\mathbf{r}) = \langle u_i(\mathbf{x})u_j(\mathbf{x})u_k(\mathbf{x}+\mathbf{r})\rangle = a r_i r_j r_k + b\,\delta_{jk} r_i + c\,\delta_{ik} r_j + d\,\delta_{ij} r_k, \tag{A1}$$

where the scalars a, b, c, and d are functions of the magnitude of the separation vector $r=\|\mathbf{r}\|$ only. Symmetry in i and j requires that $b=c$. Further, the continuity constraint $\partial \mathbb{S}_{ijk}/\partial r_k = 0$ allows the functions a, b, and d to be eliminated in terms of the third-order longitudinal correlation function,

$$f(r) = \langle v_\parallel^2(\mathbf{x}) v_\parallel(\mathbf{x}+\mathbf{r})\rangle, \tag{A2}$$

where $v_\parallel$ is the velocity component parallel to the separation vector $\mathbf{r}$. The result is

$$\mathbb{S}_{ijk}(\mathbf{r}) = \left\{ \frac{1}{2}\left(f - r\frac{df}{dr}\right)\frac{r_i r_j r_k}{r^3} + \frac{1}{4r^2}(\delta_{jk} r_i + \delta_{ik} r_j)\frac{d}{dr}(r^2 f) - \frac{f}{2r}\delta_{ij} r_k \right\}. \tag{A3}$$

The third-order longitudinal correlation function is directly related to the third-order structure function, which in the Kolmogorov inertial range is $S_3(r) = -\frac{4}{5}\epsilon r$. The correlation $f(r)$ can thus be written as

$$f(r) = \frac{S_3(r)}{6} = -\frac{2\epsilon r}{15}. \tag{A4}$$

Substituting into Eq. (A3) then immediately yields Eq. (3).

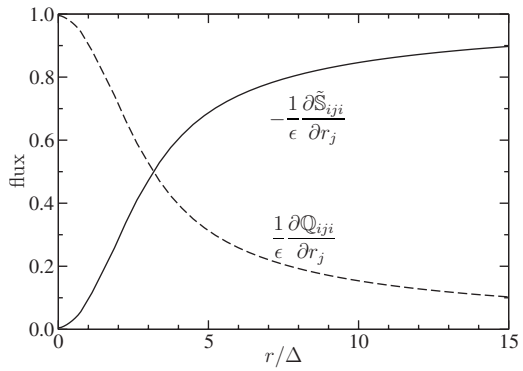

FIG. 5. The energy flux terms in Eq. (10) calculated from the third-order longitudinal structure functions in Fig. 4. Both the flux to resolved scales $-(\partial \tilde{\mathbb{S}}_{iji}/\partial r_j)$ and the flux to subfilter scales $\partial \mathbb{Q}_{iji}/\partial r_j$ are shown, normalized by ϵ.

APPENDIX B: THE MOST GENERAL FORM FOR Φ

Presented here is a condensed version of the derivation from Proudman and Reid.[15] The three-point third-order velocity correlation is $\mathbb{T}_{ijk}(\mathbf{r},\mathbf{s}) \equiv \langle v_i(\mathbf{x}) v_j(\mathbf{x}+\mathbf{r}) v_k(\mathbf{x}+\mathbf{s})\rangle$. Its Fourier transform is

$$\Phi_{ijk}(\boldsymbol{\rho},\boldsymbol{\sigma}) = i(2\pi)^{-6}\int\int \mathbb{T}_{ijk}(\mathbf{r},\mathbf{s}) e^{-i(\boldsymbol{\rho}\cdot\mathbf{r}+\boldsymbol{\sigma}\cdot\mathbf{s})} d\mathbf{r}\,d\mathbf{s}. \tag{B1}$$

Consistency with continuity requires

$$(\rho_i + \sigma_i)\Phi_{ijk}(\boldsymbol{\rho},\boldsymbol{\sigma}) = \rho_j \Phi_{ijk}(\boldsymbol{\rho},\boldsymbol{\sigma}) = \sigma_k \Phi_{ijk}(\boldsymbol{\rho},\boldsymbol{\sigma}) = 0. \tag{B2}$$

The most general isotropic third-ranked tensor function of two vectors is

$$\begin{aligned}\phi_{mnp}(\boldsymbol{\rho},\boldsymbol{\sigma}) = {} & \phi_1 \rho_m \rho_n \rho_p + \phi_2 \rho_m \rho_n \sigma_p + \phi_3 \rho_m \sigma_n \rho_p \\ & + \phi_4 \sigma_m \rho_n \rho_p + \phi_5 \sigma_m \sigma_n \sigma_p + \phi_6 \sigma_m \sigma_n \rho_p \\ & + \phi_7 \sigma_m \rho_n \sigma_p + \phi_8 \rho_m \sigma_n \sigma_p + \phi_9 \rho_m \delta_{np} \\ & + \phi_{10} \rho_n \delta_{mp} + \phi_{11} \rho_p \delta_{mn} + \phi_{12} \sigma_m \delta_{np} \\ & + \phi_{13} \sigma_n \delta_{mp} + \phi_{14} \sigma_p \delta_{mn},\end{aligned} \tag{B3}$$

where $\{\phi_1, \phi_2, \ldots, \phi_{14}\}$ are scalar functions of the magnitudes of the wavevectors $\rho \equiv |\boldsymbol{\rho}|$, $\sigma \equiv |\boldsymbol{\sigma}|$, and $\tau \equiv |\boldsymbol{\tau}|$, and $\boldsymbol{\rho} + \boldsymbol{\sigma} + \boldsymbol{\tau} = 0$.

To enforce incompressibility, we employ the divergence-free projector $\Delta_{im}(\boldsymbol{\rho}) \equiv \delta_{im} - \rho_i \rho_m / \rho^2$. So, to satisfy all three incompressibility conditions in Eq. (B2) and isotropy, we apply three projectors to ϕ_{mnp}; the result is the most general form for Φ_{ijk},

$$\Phi_{ijk}(\boldsymbol{\rho},\boldsymbol{\sigma}) = \Delta_{im}(\boldsymbol{\tau})\Delta_{jn}(\boldsymbol{\rho})\Delta_{kp}(\boldsymbol{\sigma})\phi_{mnp}(\boldsymbol{\rho},\boldsymbol{\sigma}). \tag{B4}$$

Furthermore, the triple projection operator directly eliminates all but four components of ϕ_{mnp} shown in Eq. (B3), so effectively the above equation becomes

$$\begin{aligned}\Phi_{ijk}(\boldsymbol{\rho},\boldsymbol{\sigma}) = {} & \Delta_{im}(\boldsymbol{\tau})\Delta_{jn}(\boldsymbol{\rho})\Delta_{pk}(\boldsymbol{\sigma})[\phi_3 \rho_m \sigma_n \rho_p + \phi_9 \rho_m \delta_{np} \\ & + \phi_{11} \rho_p \delta_{mn} + \phi_{13} \sigma_n \delta_{mp}].\end{aligned} \tag{B5}$$

Renaming the scalar functions as follows: $\phi_3 \to \zeta$, $\phi_9 \to \phi$, $\phi_{11} \to \phi_2$, $\phi_{13} \to \phi_1$, we obtain Eq. (16).

APPENDIX C: CALCULATION PROCEDURES

Symbolic calculation of the tensor basis functions $\mathbb{T}^n$ were carried out using a collection of scripts written in Matlab. These scripts operate on mathematical expressions in the form of strings of characters, such as `-36*DELTA_ik*r^6*s^-3*s_j*t^-3+432*r^-1*r_j*r_k*s_i*t^-1`, which is just a small part of

$\mathbb{T}^1$. Scripts perform addition, multiplication, and spatial differentiation (gradient or divergence). Addition and multiplication of terms is straightforward. Derivatives with respect to the separation vectors of scalars (e.g., r^5) and vectors (e.g., $\mathbf{r}$) must be computed. The following simple rules for the evaluation of the derivatives ∂_i^r, are implemented in the symbolic manipulation scripts, along with analogous rules for ∂_i^s and ∂_i^t:

$$\partial_i^r s^\alpha = \left.\frac{\partial s^\alpha}{\partial s_i}\right|_{\mathbf{r}} = \alpha s^{\alpha-2} s_i, \tag{C1}$$

$$\partial_i^r t^\alpha = \left.\frac{\partial t^\alpha}{\partial s_i}\right|_{\mathbf{r}} = -\alpha t^{\alpha-2} t_i, \tag{C2}$$

$$\partial_i^r s_j = \left.\frac{\partial s_j}{\partial s_i}\right|_{\mathbf{r}} = \delta_{ij}, \tag{C3}$$

$$\partial_i^r t_j = \left.\frac{\partial t_j}{\partial s_i}\right|_{\mathbf{r}} = -\delta_{ij}, \tag{C4}$$

These along with the chain rule are sufficient to evaluate Eq. (19). Finally, the scripts also simplify contractions, for example, $\delta_{ij} r_i = r_j$, $r_j s_j = \mathbf{r}\cdot\mathbf{s}$, and $s_j s_j = s^2$.

Using the symbolic evaluator described above, Eq. (19) was evaluated for 20 different ψ given by $\psi = p_{a,b} \equiv (r^a s^b - r^b s^a) t^c$, where $a+b+c=8$ and a, b, $c \geq 0$ are integers. Of these 20 candidate tensor expressions, 14 are nonzero. However, all 14 have discontinuities and/or singularities (which are nonphysical) at r, s, or t of zero.

To eliminate the discontinuities and singularities, linear combinations of the 14 nontrivial basis functions are sought which exactly cancel them. This is done by using the first order approximation of $\mathbf{t}$ for small s, namely, $\mathbf{t} \approx \mathbf{r}$ and simplifying the resulting expressions for each basis function. Singular and discontinuous terms (for small s) are identified as those with net power of s that is less than or equal to zero, and that are not independent of s. Thus, terms with factors such as s_k/s or $s_i s_j s_k / s^3$ are identified as discontinuous at $s=0$ (their limiting values as $s \to 0$ depend on the direction of the approach), while factors such as s_k/s^3 and $1/s$ are simply singular at $s=0$. Each of the 14 reduced basis tensors includes one or more of 28 distinct discontinuous or singular terms. The null space of the 28×14 matrix of coefficients of the singular and discontinuous terms defines the space of the tensor function in which all these terms cancel. Remarkably, it was found that the dimension of this null space is six (rather than zero). A vector basis for the null space then defines a basis of tensor functions in which the problematic terms have been eliminated.

However, this does not necessarily lead to a basis in which there are no singularities or discontinuities. The reason is that the approximation for $\mathbf{t}$ was only first order in s, and higher order terms can also lead to singularities or discontinuities. Indeed, it was observed that 4 of the 6 basis tensors determined above were discontinuous. By substituting $\mathbf{t}=\mathbf{r}-\mathbf{s}$, and expanding to explicitly expose the higher-order terms in s, the remaining singular/discontinuous terms were identified. Using the same procedure described above, it was found that these singularities and discontinuities had a five-dimensional null-space. A basis for the five-dimensional space of continuous nonsingular model tensors is thus found and is given in Eqs. (32)–(36).

[1] U. Frisch, *Turbulence: The Legacy of A. N. Kolmogorov* (Cambridge University Press, Cambridge, 1995).
[2] S. B. Pope, *Turbulent Flows* (Cambridge University Press, Cambridge, 2000).
[3] R. Kraichnan, "The structure of isotropic turbulence at very high Reynolds numbers," J. Fluid Mech. **5**, 497 (1959).
[4] R. H. Kraichnan, "Direct interaction approximation for shear and thermally driven turbulence," Phys. Fluids **7**, 1048 (1964).
[5] J. Chollet and M. Lesieur, "Parameterization of small scales of three-dimensional isotropic turbulence using spectral closures," J. Atmos. Sci. **38**, 2747 (1981).
[6] M. Lesieur, *Turbulence in Fluids*, 3rd ed. (Kluwer Academic, Dordrecht, 1997).
[7] J. O'Neil and C. Meneveau, "Spatial correlations in turbulence: Predictions from the multifractal formalism and comparison with experiments," Phys. Fluids A **5**, 158 (1993).
[8] J. Qian, "Closure approach to high-order structure functions of turbulence," Phys. Rev. Lett. **84**, 646 (2000).
[9] L. Shao, Z. Zhang, G. Cui, and C. Xu, "Subgrid modeling of anisotropic rotating homogeneous turbulence," Phys. Fluids **17**, 115106 (2005).
[10] T. von Karman and L. Howarth, "On the statistical theory of isotropic turbulence," Proc. R. Soc. London, Ser. A **164**, 192 (1938).
[11] A. N. Kolmogorov, "Dissipation of energy in locally isotropic turbulence," Dokl. Akad. Nauk SSSR **32**, 16 (1941); reprinted in Proc. R. Soc. London, Ser. A **434**, 15 (1991).
[12] J. Langford and R. Moser, "Optimal LES formulations for isotropic turbulence," J. Fluid Mech. **398**, 321 (1999).
[13] P. S. Zandonade, J. A. Langford, and R. D. Moser, "Finite volume optimal large-eddy simulation of isotropic turbulence," Phys. Fluids **16**, 2255 (2004).
[14] J. A. Langford and R. D. Moser, "Optimal large-eddy simulation results for isotropic turbulence," J. Fluid Mech. **521**, 273 (2004).
[15] I. Proudman and W. H. Reid, "On the decay of a normally distributed and homogeneous turbulent velocity field," Philos. Trans. R. Soc. London, Ser. A **247**, 163 (1954).
[16] A. N. Kolmogorov, "The local structure of turbulence in incompressible viscous fluid for very large Reynolds number," C. R. Acad. Sci. URSS **30**, 301 (1941); reprinted in Proc. R. Soc. London, Ser. A **434**, 9 (1991).
[17] Y. Kaneda, T. Ishihara, M. Yokokawa, K. Itakura, and A. Uno, "Energy dissipation and energy spectrum in high resolution direct numerical simulations of turbulence in a periodic box," Phys. Fluids **15**, L21 (2003).
[18] Y. Tsuji, "Intermittency effect on energy spectrum in high-Reynolds number turbulence," Phys. Fluids **16**, L43 (2004).
[19] K. R. Sreenivasan and R. A. Antonia, "The phenomenology of small-scale turbulence," Annu. Rev. Fluid Mech. **29**, 435 (1997).
[20] See EPAPS Document No. E-PHFLE6-19-017710 for data explicitly defining the model expressions and a program to evaluate the model numerically. This document can be reached through a direct link in the online article's HTML reference section or via the EPAPS homepage (http://www.aip.org/pubservs/epaps.html).